Quasi-Static Analysis of an Optically Illuminated Directional Coupler

A. M. E. Safwat, *Student Member, IEEE,* D. A. M. Khalil, H. Elhennawy, and H. F. Ragaie, *Member, IEEE*

***Abstract*— In this paper, we present the analysis of an optically illuminated directional coupler using a quasi-static technique. Closed-form expressions of the matching conditions in both the dark and illuminated states are developed. The results obtained by our analytical model are in good agreement with the experimental results as well as those obtained by the monolithic microwave integrated-circuit analysis and design simulator (MMICAD). A discussion of the effects of the parameter variations are also included.**

***Index Terms*—Directional coupler, optically illuminated, sliding tuner.**

I. Introduction

The field of optically controlled microwave devices has shown a remarkable progress in the last decade [1]–[3]. We have recently proposed the use of the illuminated directional coupler as a variable-tuned matched load [4]. In this application, the basic idea is based on the use of ports 2 and 3 as open- or short-circuit stubs which are connected nearly in parallel. The optical spot creates a variable resistance between the coupled microstrip lines. The value of this resistance is controlled by the optical intensity while its location is controlled by the position of the optical spot. Thus, by moving the optical spot, we effectively control the lengths of the equivalent stubs connected in parallel with the load. Thus, we have an effective sliding spot tuner that can be used to achieve matching at the required frequency, as will be shown.

In this paper, we present the analysis of this optically controlled structure using the transmission matrices based on the quasi-static technique. Closed-form expressions for the matching conditions in both the dark and illuminated states are developed. The results obtained by the developed model are in good agreement with those obtained by the experimental results, as well as the monolithic microwave integrated-circuit analysis and design simulator (MMICAD).

II. Theory

When light is incident on the gap between the two coupled lines shown in Fig. 1, a surface resistance R is created. As

Manuscript received November 28, 1996; revised April 24, 1997.

A. M. E. Safwat was with Ain Shams University, Faculty of Engineering, Electronics and Communication Engineering Department, Abbasia, Cairo, Egypt. He is now with the Electrical Engineering Department, University of Maryland at College Park, College Park, MD 20742 USA.

D. A. M. Khalil, H. Elhennawy, and H. F. Ragaie are with Ain Shams University, Faculty of Engineering, Electronics and Communication Engineering Department, Abbasia, Cairo, Egypt.

Publisher Item Identifier S 0018-9480(97)05994-2.

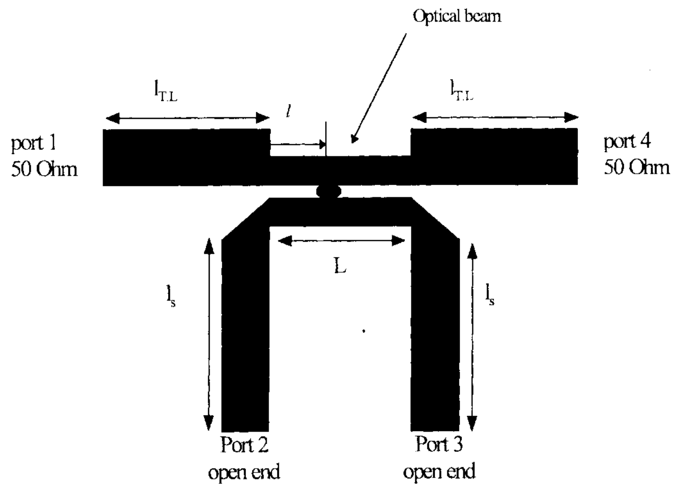

Fig. 1. The structure proposed for the optically controlled matched load, two coupled lines of width $w$and separation s, connected to four transmission lines of width w.

a result, it becomes more convenient to consider the two coupled lines as if they are divided into three sections. These three, along with the four transmission lines, form the seven sections of the overall structure shown in Fig. 2. Thus, each section can be represented by its own transmission matrix. Sections II and IV are simple coupled microstrip lines of lengths l and $L - l$, respectively. Section 3 corresponds to the resistor created by incident light while the other four sections are simply four transmission lines with characteristic impedance Z_c. For the coupled microstrip line of length l, the Z matrix elements are given in [5], [6]. Using the symmetry of the Z matrix and interchanging the variables such that the input voltages and currents can be written as a function of the output voltages and currents, an equivalent transmission matrix similar to the $ABCD$ matrix of the two-port network can be derived. Knowing the transmission matrix for each section [7], the two-port equivalent of Sections II–IV, VI, and VII can now be obtained after replacing ports 2 and 3 by their equivalent impedances Z_2 and Z_3, respectively, and thus the transmission matrix for the whole system can be obtained. Knowing the $ABCD$ matrix of the system, the S-parameters can be calculated in both the dark and illuminated states [7]. Further approximation can be used to get closed-form expressions for the matching conditions of the structure in both states. This is discussed in the following sections.

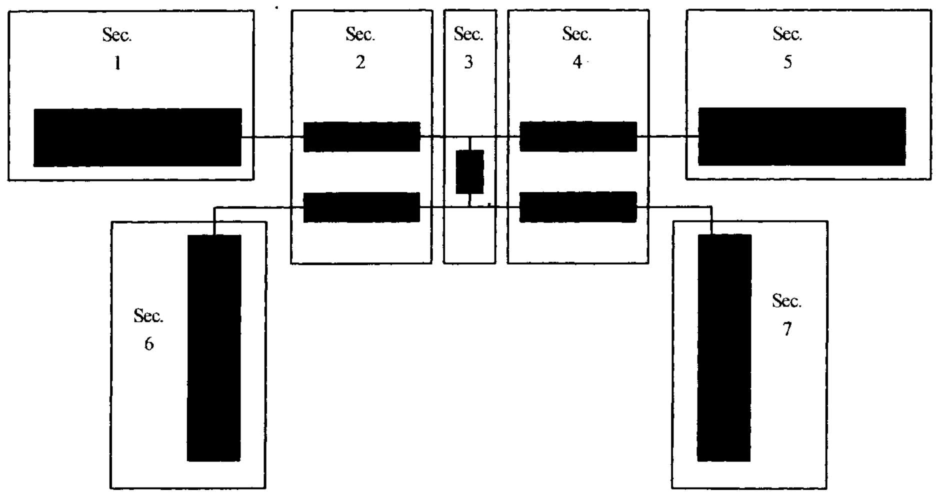

Fig. 2. The equivalent seven sections for the structure shown in Fig. 1.

A. Dark State

To get a closed-form expression for the matching conditions of the structure in the dark state, we put $G = 0$, neglect the dispersion effect, and assume that the even- and odd-mode propagation constants of the microstrip coupled lines are equal, then we calculate the $ABCD$ matrix of the coupled lines connected to the two stubs. The minimum in S_{11} occurs when the input impedance equals Z_c. Assuming that the output port is terminated by Z_c, and after a straightforward mathematical analysis, it can be easily demonstrated that the minimum in S_{11} (matching condition) can be achieved only if $Z_2 = Z_3$, i.e., the two stubs have the same length l_s and

$$\sin\theta\Bigg\{\cos\theta\left[(Z_e+Z_o)\left(1-\frac{Z_c^2}{Z_eZ_o}\right)\right] + \sin\theta\left[\frac{1}{4\tan\theta_s}\left(\frac{Z_c}{Z_eZ_o}(Z_e+Z_o)^2-\frac{4Z_c^3}{Z_eZ_o}\right) + \frac{\tan\theta_s}{4}\left(\frac{Z_c}{Z_eZ_o}(Z_e+Z_o)^2-\frac{4Z_eZ_o}{Z_c}\right)\right]\Bigg\} = 0 \quad (1)$$

where Z_e and Z_o are the characteristic impedances of the even and odd modes, respectively. To get the three roots of (1), the coupled lines should be designed such that

$$\frac{2Z_eZ_o}{Z_e+Z_o} > Z_c \quad \text{and} \quad (Z_e+Z_o) > 2Z_c$$

or

$$\frac{2Z_eZ_o}{Z_e+Z_o} < Z_c \quad \text{and} \quad (Z_e+Z_o) < 2Z_c. \quad (2)$$

Substituting with $L = 4.7$ mm, $w' = 155$ μm, $s = 50$ μm, $w = 410$ μm, $l_s = 4.3$ mm, and $L_{tl} = 4$ mm, in the empirical formula given in [7], [8], we get: $Z_c = 49.7$ Ω, $\varepsilon_{\text{eff}} = 7.69$, $Z_e = 103.8$ Ω, $Z_o = 34.4$ Ω, $\varepsilon_{\text{eff}}^e = 7.64$, and $\varepsilon_{\text{eff}}^o = 6.44$ where $\varepsilon_{\text{eff}}^e$ and $\varepsilon_{\text{eff}}^o$ are the even- and odd-mode effective permittivity for the coupled line. Using (1), a minimum in S_{11} is obtained at frequency $f = 11.5$ GHz corresponding to $\theta = \pi$. The two other minima are obtained at the frequencies 5.1 and 7.1 GHz, respectively. The exact S_{11} is then calculated, taking dispersion into consideration and neglecting both conductor and dielectric loss. The results are compared to those obtained by the MMICAD simulator, as shown in Fig. 3. We can see that the same qualitative behavior is obtained and that the developed approximate technique can be used to predict the structure performance. In the same time, there is a little deviation in the propagation constant between the two results (model, MMICAD). This is due to the fact that the empirical equation for the dispersion effect considered in MMICAD is not well defined in the literature. Fig. 4 shows the input impedance of the coupled lines as a function of frequency. It is clear that Z_{in} has three points where its value equals 50 Ω. These points correspond to the minima in S_{11}. It is important to note here that between 3.8 and 8.2 GHz, i.e., between its two maxima value, the input impedance is nearly equal to 50 Ω. By inserting a resistor between the coupled lines, one can adjust the input impedance such that the reflection is eliminated in this range of frequencies. This will be shown in the illuminated state. It should also be noted that

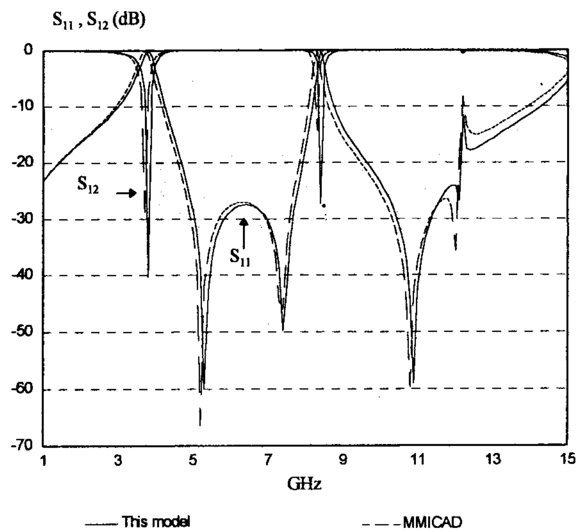

Fig. 3. S_{11} and S_{12} obtained by the model compared with those obtained by the MMICAD simulator. The losses are neglected.

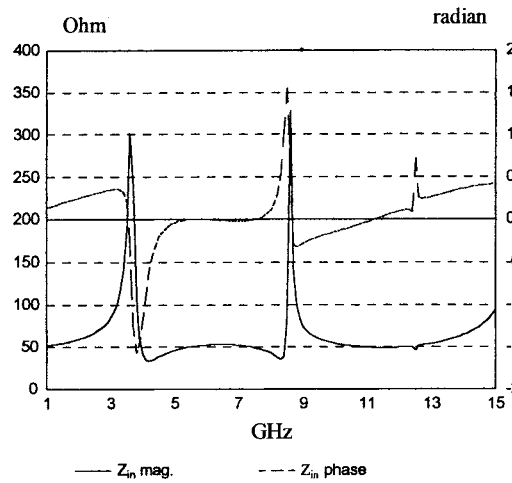

Fig. 4. The frequency response of the coupled lines impedance with a load equals 50 Ω.

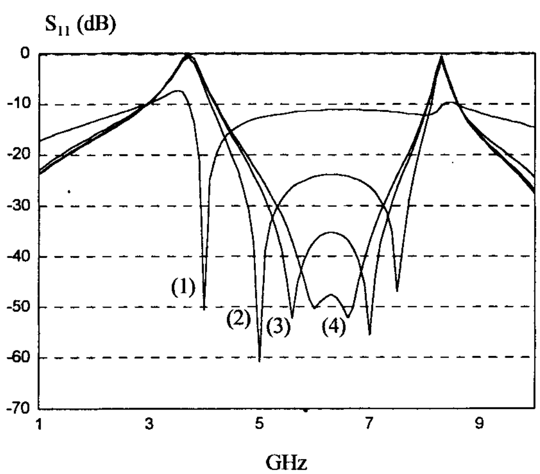

Fig. 5. S_{11} under illumination by a spot of intensity corresponding to a resistance R and position l, (1) $l = 4.2$ mm, $R = 62$ Ω. (2) $l = 4.7$ mm, $R = 785$ Ω. (3) $l = 0.1$ mm, $R = 700$ Ω. (4) $l = 0.1$ mm, $R = 874$ Ω.

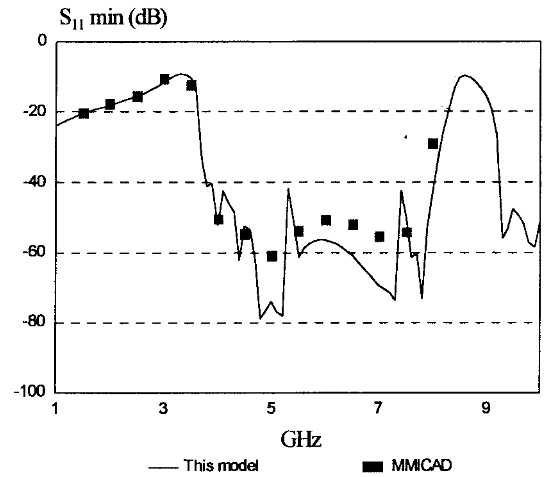

(a)

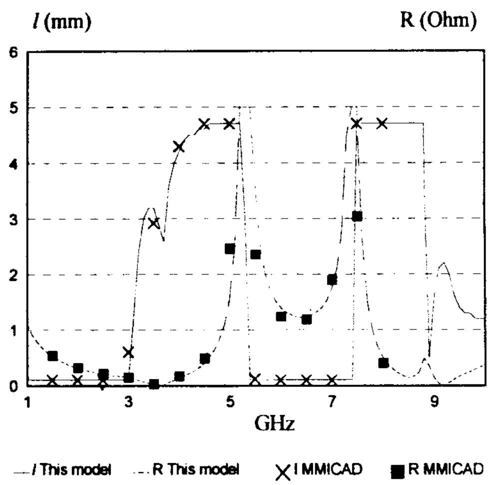

(b)

Fig. 6. (a) The minimum value for S_{11} which can be achieved compared with those obtained by the MMICAD simulator. (b) The values of the resistor and their position required to achieve this minimum compared to those obtained by the MMICAD simulator.

when substituting by the conventional operating conditions of the backward directional coupler, i.e., $Z_c^2 = Z_e Z_o$, (1) will have imaginary roots. This can not be accepted since it is previously assumed that β has only positive values. This shows that the conventional design of the backward directional coupler can not be used to achieve the required matching conditions.

B. Illuminated State

Fig. 5 shows the calculated S_{11} of the structure, when light is *on* for different powers and positions of the optical spot. From these results, we see that S_{11} of the structure under illumination has a very strong frequency dependence. At a certain frequency, the reflection from the illuminated directional coupler is minimized to less than −50 dB in a notch behavior. Fig. 5 also shows the possibility of tuning the structure by simply changing the optical spot intensity and position as previously shown in [4].

To determine the tuning range in which a minimum for S_{11} can be obtained at a certain frequency, we fix the frequency and vary the value of the resistor and its position between the coupled lines until the minimum is obtained. Fig. 6(a) shows the minimum value for S_{11} while Fig. 6(b) shows the values of the resistor and their position required to get this minimum. Fig. 6(a) and (b) should be read simultaneously, i.e., for a certain frequency. Fig. 6(a) shows the lowest value for S_{11} that can be achieved while Fig. 6(b) shows the value of the resistor and the position required to achieve this minimum. These results are also compared to those obtained by the MMICAD simulator with good agreement observed. The little difference may be due to: 1) dispersion evaluation as previously discussed, where the dispersion calculation is not well defined in the MMICAD simulator and 2) in the simulator we model the photoresistance as a thin-film resistor of dimensions 50 μm $*$ 50 μm, while in this model we use a simple resistor with the equivalent value. As we have done in the dark state, simple design equations can be developed in the illuminated state. Assuming that the even and odd propagation constants are equal and neglecting dispersion, the matching condition is given by the two following coupled equations:

$$
\begin{aligned}
&Z_c G_{\mathrm{ph}} \bigg(\frac{Z_c Z_o \cos^2\theta_1 \sin 2(\theta-\theta_1)}{\tan\theta_s} \\
&\quad - \frac{\tan\theta_s Z_o^3 \sin^2\theta_1 \sin 2(\theta-\theta_1)}{Z_c} \bigg) \\
&\quad = Z_c^2 \cos\theta_1 \cos(2\theta-\theta_1) + Z_o^2 \sin(\theta-\theta_1)\sin(\theta+\theta_1) \\
&\quad + Z_c^2 \cos\theta_1 \cos\theta \cos(\theta-\theta_1) \\
&\quad - Z_c^2 \frac{Z_o}{Z_e} \sin\theta_1 \sin\theta \cos(\theta-\theta_1) \\
&\quad + Z_o Z_e \sin\theta \sin\theta_1 \cos(\theta-\theta_1) \\
&\quad - \frac{\tan\theta_s}{Z_c} \sin\theta \bigg\{ \frac{Z_c^2(Z_e+Z_o)}{2} \cos\theta_1 \cos(\theta-\theta_1) \\
&\quad - \frac{Z_c^2(Z_e+Z_o)Z_o}{2Z_e} \sin\theta_1 \sin(\theta-\theta_1) \\
&\quad + 2Z_o^3 \sin\theta_1 \sin(\theta-\theta_1) \bigg\} \\
&\quad + \frac{Z_c \sin\theta}{\tan\theta_s} \bigg\{ \frac{2Z_c^2}{Z_e} \cos\theta_1 \cos(\theta-\theta_1) \\
&\quad - \frac{(Z_e+Z_o)}{2} \cos\theta_1 \cos(\theta-\theta_1) \\
&\quad + \frac{(Z_e+Z_o)Z_o}{2Z_e} \sin\theta_1 \sin(\theta-\theta_1) \bigg\}
\end{aligned} \tag{3a}
$$

$$
\begin{aligned}
&G_{\mathrm{ph}}^2 \bigg[Z_o Z_c^2 \cos^2\theta_1 \sin 2(\theta-\theta_1) + Z_c^3 \sin^2\theta_1 \sin 2(\theta-\theta_1) \\
&\quad - \frac{\tan\theta_s}{2} Z_c Z_o^2 \sin 2\theta_1 \sin 2(\theta-\theta_1) \\
&\quad - \frac{Z_c}{2\tan\theta_s} Z_o^2 \sin 2\theta_1 \sin 2(\theta-\theta_1) \bigg] \\
&\quad - Z_c G_{\mathrm{ph}} \bigg[2Z_o \cos\theta \sin(\theta-2\theta_1) \\
&\quad - \frac{\tan\theta_s}{Z_c} Z_o \sin\theta \{ Z_o \cos\theta_1 \sin(\theta-\theta_1) \\
&\quad - Z_e \sin\theta_1 \cos(\theta-\theta_1) \} \\
&\quad + \frac{Z_c}{\tan\theta_s} \sin\theta \bigg\{ \cos\theta_1 \sin(\theta-\theta_1) \\
&\quad + \frac{Z_o}{Z_e} \sin\theta_1 \cos(\theta-\theta_1) \bigg\} \bigg] \\
&\quad + (Z_e+Z_o) \sin\theta \cos\theta \bigg\{ \frac{Z_c^2}{Z_e Z_o} - 1 \bigg) \\
&\quad + \frac{\tan\theta_s}{Z_c} \bigg\{ \frac{Z_c^2(Z_e+Z_o)^2}{4Z_e Z_o} \sin^2\theta + \frac{Z_e Z_o}{Z_c} \sin^2\theta \bigg\} \\
&\quad + \frac{Z_c}{\tan\theta_s} \bigg\{ \frac{Z_c^2}{Z_e Z_o} \sin^2\theta - \frac{(Z_e+Z_o)^2}{4Z_e Z_o} \sin^2\theta \bigg\} = 0
\end{aligned} \tag{3b}
$$

where θ is the total electrical length of the coupled lines and θ_1 is the electrical length calculated from the beginning of the coupled line to the position of the created photoconductance. Solving these two equations, we can determine the value of the created photoconductance and its position required for matching at port 1. However, before solving them, we may observe that (3b) is a second-order equation with two roots. This explains the two minima which appear in S_{11} for the same value of l and R in Fig. 5.

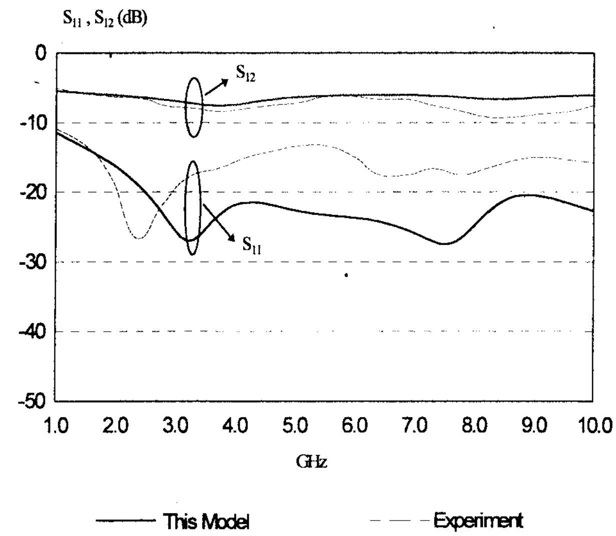

Fig. 7. Measured and calculated S parameters of the proposed structure without illumination. The metal strip on the surface is the aluminum $\rho = 2.75 * 10^{-8}$ Ωm and silicon substrate of resistivity $= 1$ Ωm corresponding to tangent loss $*$ frequency (GHz) $= 1.5$.

We have also studied the effect of varying the load at port 2. For different values of this load, matching at the required frequency could be achieved when the proper values of l and R (optical power) are chosen. Between 1 and 10 GHz, and due to the fixed length of the coupled lines, tuning can be obtained in separate ranges of frequencies. As the load approaches 50 Ω, these ranges merge together. Also, to obtain a minimum in S_{11}, the value of the resistor is relatively small (less than 20 Ω) which means a high-incident optical power. However, as the electron–hole pair concentration increases, the lifetime is reduced and the value of the created resistor tends to saturate. Thus, it might be quite difficult to obtain all the values of the resistor as in the simulation, and we can predict that the practical tuning range is smaller than the simulated one.

III. Comparison with Experimental Results and Discussion

In this section, we compare the results of our model to those experimentally obtained and previously published in [4]. The experimental setup is described in details in [4], [9].

Since we are considering silicon substrates, the effect of the losses should also be taken into account. The expressions for the conductor and dielectric losses for single- and double-microstrip transmission lines are given in [7].

For semiconductor loss evaluation, the silicon substrate is represented by its tangent loss given by $\varepsilon''/\varepsilon'$, where ε' and ε'' are the real and the imaginary parts of the permittivity. They are calculated using the plasma-oscillation frequency described in [10], which gives [4]

$$\varepsilon''/\varepsilon' = 1.5/\text{freq. (GHz)} \tag{4}$$

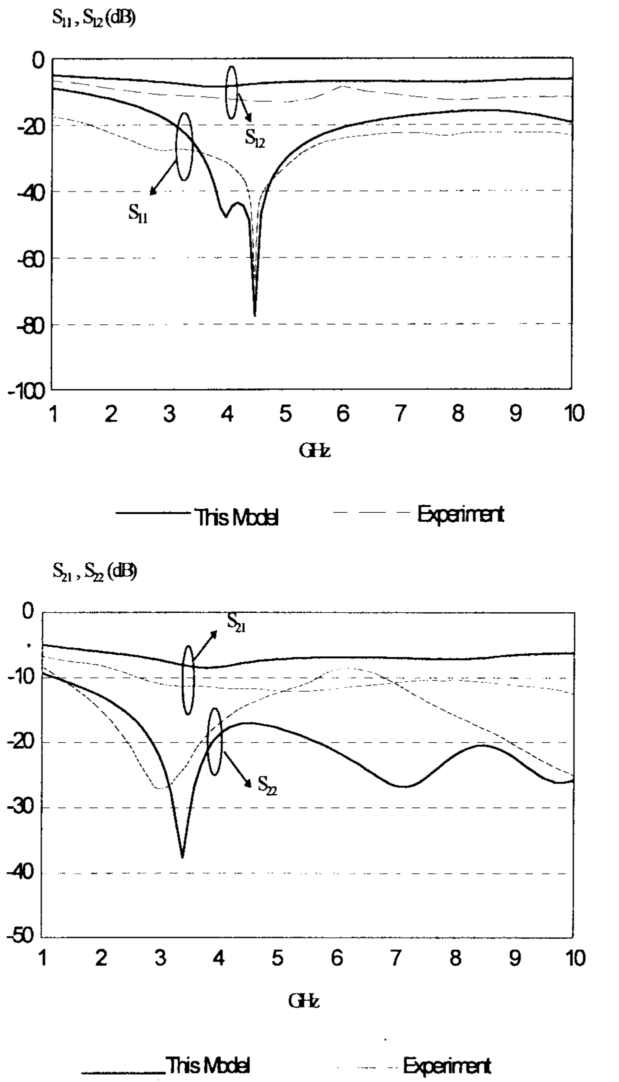

Fig. 8. The $4S$-parameters of the illuminated directional coupler experimentally at $l = 3.5$ mm, $P = 420$ mW, theoretically at $l = 3.9$ mm, $R = 111\Omega$.

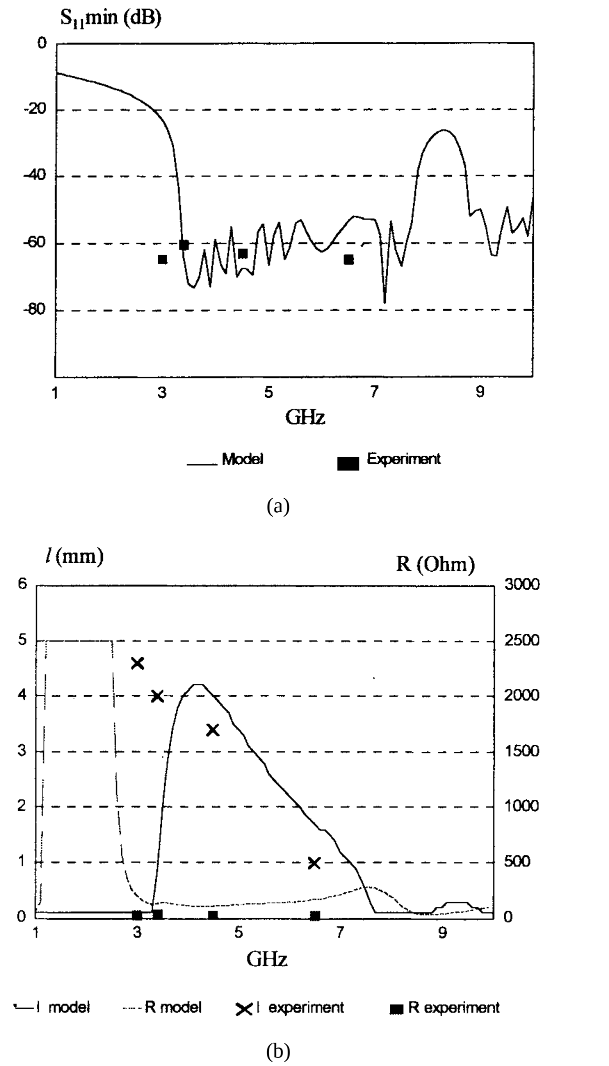

Fig. 9. (a) The minimum value for S_{11} which can be achieved. (b) The values of the resistor and its position required to achieve this minimum. Theoretical results are calculated for tangent loss $*$ frequency (GHz) $= 1.5$, and metal strip on the surface is Al of thickness 0.4 μm.

where the variation in the real part of the relative permittivity is found to be negligible. The conductor losses are expressed by the resistivity of the aluminum strip on the surface which is taken equal to $2.75 * 10^{-8}$ Ω·m.

A. Dark State

Fig. 7 shows the measured and calculated S-parameters of the structure in the dark state. S_{11} (S_{22}) is approximately -11 dB at 1-GHz frequency. The two minima observed in the dark-state performance are well explained by the matching conditions obtained in (1). A good agreement is also observed between the exact solution and the practical measurements. The difference between experiment and theory may be due to: 1) the inaccuracy in the calculation of the substrate losses where the last are functions of the depth—i.e., the resistivity on the surface differs from that in the bulk of the substrate, as $\rho = 100$ Ω·cm is measured on the surface and not in bulk, a certain error in the losses predictions may take place and 2) the effect of losses on the characteristic impedance—for small losses, the characteristic impedance can be calculated using the expressions given in [7], [8]. In our case, we have used the same expressions for high dielectric losses.

B. Illuminated State

Fig. 8 shows the experimental and theoretical $4S$-parameters of the device under illumination when matching is achieved at frequency equals 4.5 GHz. As we can see, S_{11} exhibits a strong frequency dependent behavior while S_{21} is found to be nearly constant. In the model, the illumination does not affect S_{21}, i.e., the power is absorbed by the created photoresistor, experimentally the illumination results in a reduction of S_{21} by about 4 dB at all frequencies.

Fig. 9 shows a comparison between the theoretical results and those obtained experimentally [4]. While an experimental tuning range from 3.0 to 6.7 GHz has been obtained, the theoretical one extents from 3.4 to 7.7 GHz. Fig. 9(b) shows

TABLE I
COMPARISON BETWEEN THEORETICAL AND EXPERIMENTAL RESULTS UNDER DIFFERENT OPERATING CONDITIONS

State			Results of S11	
Port 2	**Stub 1**	**Stub 2**	**Theory**	**Experiment**
50 Ohm	Open circuit (O.C.)	Open circuit (O.C.)	Variable scan 3.4 GHz - 7.7 GHz	Variable scan 3 GHz - 6.4 GHz
75 Ohm	O.C.	O.C.	Variable scan in ranges: [3.4 GHz -3.8 GHz], [4.6 GHz -8.1 GHz], [9.2 GHz -9.7 GHz]	Discrete frequencies: 3.07 GHz, 3.4 GHz, 4.5 GHz, 6.35 GHz.
Short circuit	O.C.	O.C.	Variable scan [2.6 GHz -6.8 GHz]	Two frequencies 3.94 GHz, 6.37 GHz
Open circuit	O.C.	O.C.	Variable scan [5.6 GHz -10.0 GHz]	Two frequencies 3.07 GHz , 5.65 GHz
50 Ohm	Short Circuit (S.C.)	Short Circuit (S.C.)	Variable scan [6.0 GHz -6.9 GHz]	Two frequencies 2.9 GHz, 6.6 GHz

the approximate values for the spot position and the incident power (the created photoresistor). From this figure, we can see that the relation between the length l indicating the position of the spot and the frequency is inversely proportional, i.e., for low matching frequency, the spot should be placed near to the end of the coupled lines and vice versa.

A summary of the theoretical results compared to those practically obtained is shown in Table I. Port 1 is the input port, where port 2 and the two stubs have different conditions as stated in the table. The behavior mentioned is that of S_{11}. As we can see, this table shows good agreement between the theoretical and experimental results.

IV. CONCLUSION

In this paper, we have presented the analysis of an optically controlled directional coupler that can be used as reflection filter. The suggested operating point for the design of this directional coupler is different from the normal backward directional coupler. When such a coupler is used in the dark state it enables three points of matching to be obtained, depending on the coupler and stub lengths. When the coupler is illuminated, its reflection coefficient shows a notch behavior with a value down to -50 dB at a specific frequency. This frequency can be controlled by varying both the incident power and the position of the incident spot. A wide tuning range has been predicted by this technique. The theoretical results are compared to numerical results obtained by the MMICAD simulator and good agreement is obtained. Closed-form approximate expressions for the matching conditions in both the dark and illuminated states are also developed. The comparison with exact solutions shows reasonable qualitative agreement.

Comparison between the theoretical predictions and the experimental results shows that a good qualitative agreement is obtained for the structure with different operating condition. Quantitatively, a small deviation in the values of the matching frequencies is observed. This might be an inaccuracy in the determination of the substrate dispersion. The transition between the flange-mount jack receptacle connector and the microstrip transmission line also affects the experimental results at high frequency. However, in the $X-C$ band, the developed model and the approximate design equations can be used to give quite reasonable results.

ACKNOWLEDGMENT

The authors would like to thank Prof. S. Tedgini and Dr. A. Vilcot from the LEMO-INPG, Grenoble France, for their great assistance in the experimental part considered in this paper.

REFERENCES

[1] R. Simons, *Optical Control of Microwave Devices*. Norwood, MA: Artech House, 1990.
[2] H. Shimasaki and M. Tsutsumi, "Light-controlled microstrip line coupler," *Int. J. Infrared Millimeter Waves*, vol. 10, no. 9, pp. 1131–1138, 1989.
[3] I. Anderson, "High speed microwave switching using laser-controlled microstrip directional coupler," *Electron. Lett.*, vol. 25, no. 5, pp. 386–369, Mar. 1989.
[4] A. M. E. Safwat, J. Haider, D. A. M. Khalil, M. Bouthinon, H. Elhennawy, and H. F. Ragaie, "An optically controlled matching technique," *Microwave Opt. Technol. Lett.*, vol. 11, no. 5, pp. 284–290, Apr. 1996.
[5] K. C. Gupta, R. Garg, and I. Bahl, *Microstrip Lines and Slotlines*. Norwood, MA: Artech House, 1979.
[6] T. Itoh, *Planar Transmission Line Structures*. Piscataway, NJ: IEEE Press, 1987.
[7] E. H. Fooks and R. A. Zakarevicius, *Microwave Engineering Using Microstrip Circuits*. Englewood Cliffs, NJ: Prentice-Hall, 1990.
[8] T. C. Edwards, *Foundations for Microstrip Circuit Design*. New York: Wiley, 1981.

[9] J. Haidar, A. M. E. Safwat, A. Vilcot, S. Tedjni, and M. Bouthinon, "Etude experimental de l'illumination optique sur un coupleur en microruban sur silicium," in *Neuviemes Journees Nationales Microondes*, Paris, France, Apr. 4–6, 1995.

[10] C. H. Lee, P. S. Mak, and A. P. Defonzo, "Optical control of millimeter-wave propagation in dielectric waveguides," *IEEE, J. Quantum Electron.*, vol. QE-16, pp. 277–287, Mar. 1980.

A. M. E. Safwat (S'91) was born in Cairo, Egypt, on May 30, 1970. He received the B.Sc. degree with honors and the M.Sc. degree, both in electrical engineering, from Ain-Shams University, Cairo, Egypt, in 1993 and 1996, respectively. He is currently working toward the Ph.D. degree at the University of Maryland at College Park.

From 1993 to 1997, he was a Teaching Assistant at Ain-Shams University.

D. A. M. Khalil was born in Cairo, Egypt, in September, 1961. He received the B.Sc. (with honors) and the M.Sc. degrees, both in electrical engineering, from Ain-Shams University, Cairo, Egypt, in 1984 and 1988, respectively.

From 1984 to 1988, he was a Teaching Assistant at Ain-Shams University. While there, he was engaged in research in the linewidth of semiconductor lasers. In 1988, he joined the Laboratoire d'Electromagnetisme Microondes et Optoelectronique (LEMO-URA CNRS), Grenoble, France. His recent work has centered in high-speed optoelectronics and modeling of the propagation in integrated optical circuits. Since 1993, he has been an Assistant Professor at Ain-Shams University.

Dr. Khalil is a member of SPIE and the Topical Society of Laser Science, Egypt.

H. Elhennawy, photograph and biography not available at the time of publication.

H. F. Ragaie, (M'96) photograph and biography not available at the time of publication.